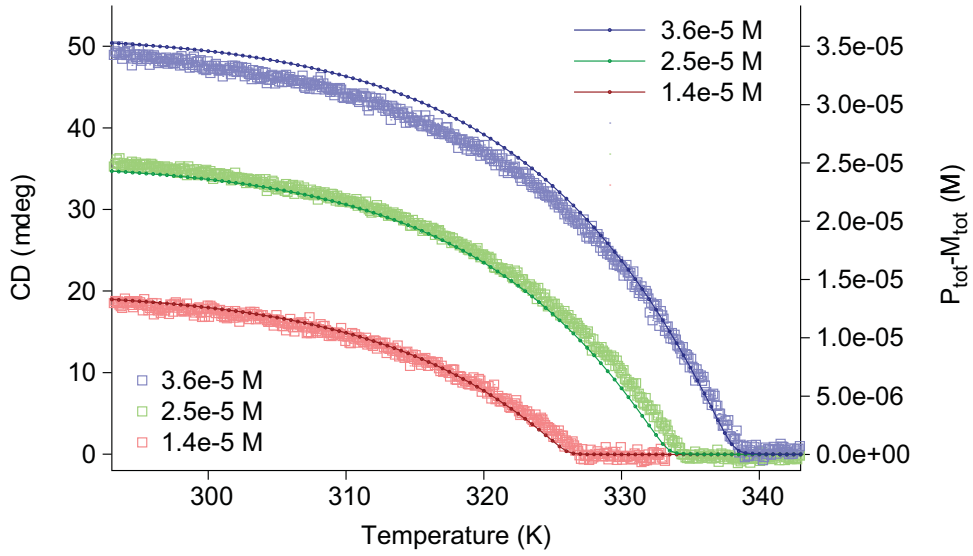

Supplementary Figure S1| Fit of experimental melting curves for (*R*)-1 in MCH. Comparison of the experimentally determined CD at 223 nm (symbols) as a function of temperature[28] to the total concentration of BTA (*R*)-**1** molecules present in all oligomers and polymers with length two or higher calculated using the mass-balance model (lines).

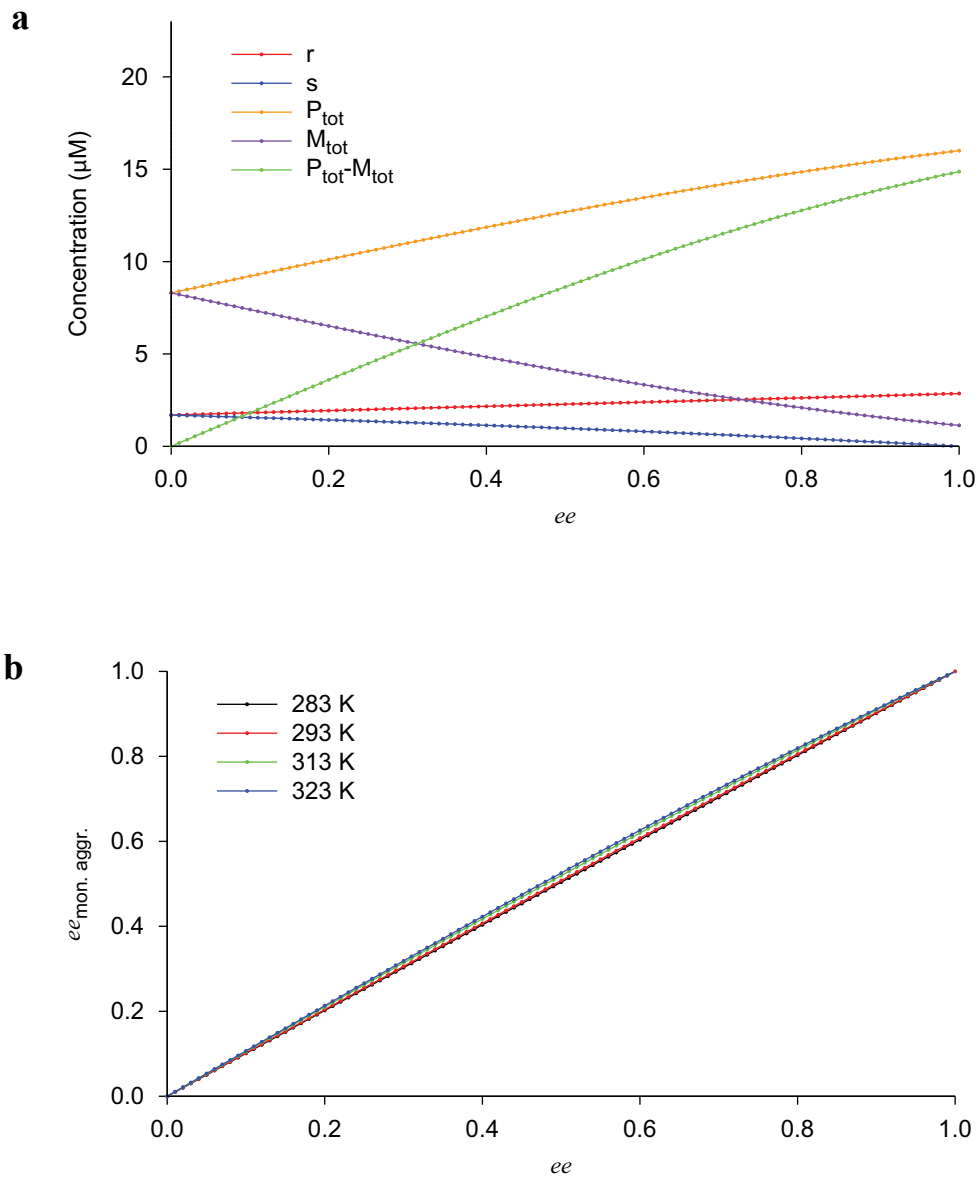

Supplementary Figure S2| Majority-rules results for isodesmic supramolecular copolymerization. The thermodynamic parameters and concentration are equivalent to those in Figures 4c and 5b except for the nucleation penalty ΔH^0_{NP} which equals zero for isodesmic supramolecular polymerizations. (**a**) Computed speciation plot for an isodesmic supramolecular copolymerization instead of the cooperative supramolecular copolymerization as in Figure 4c. In case of such an isodesmic supramolecular copolymerization there is no critical *ee*. (**b**) Enantiomeric excess of monomers present in aggregates ($ee_{mon.\ aggr.}$) computed as a function of *ee* for an isodesmic supramolecular copolymerization instead of the cooperative supramolecular copolymerization as in Figure 5b. The strong enantiomeric enrichment of monomers present in aggregates with respect to the original solution, which was observed for the cooperative supramolecular polymerizations, is lacking here.

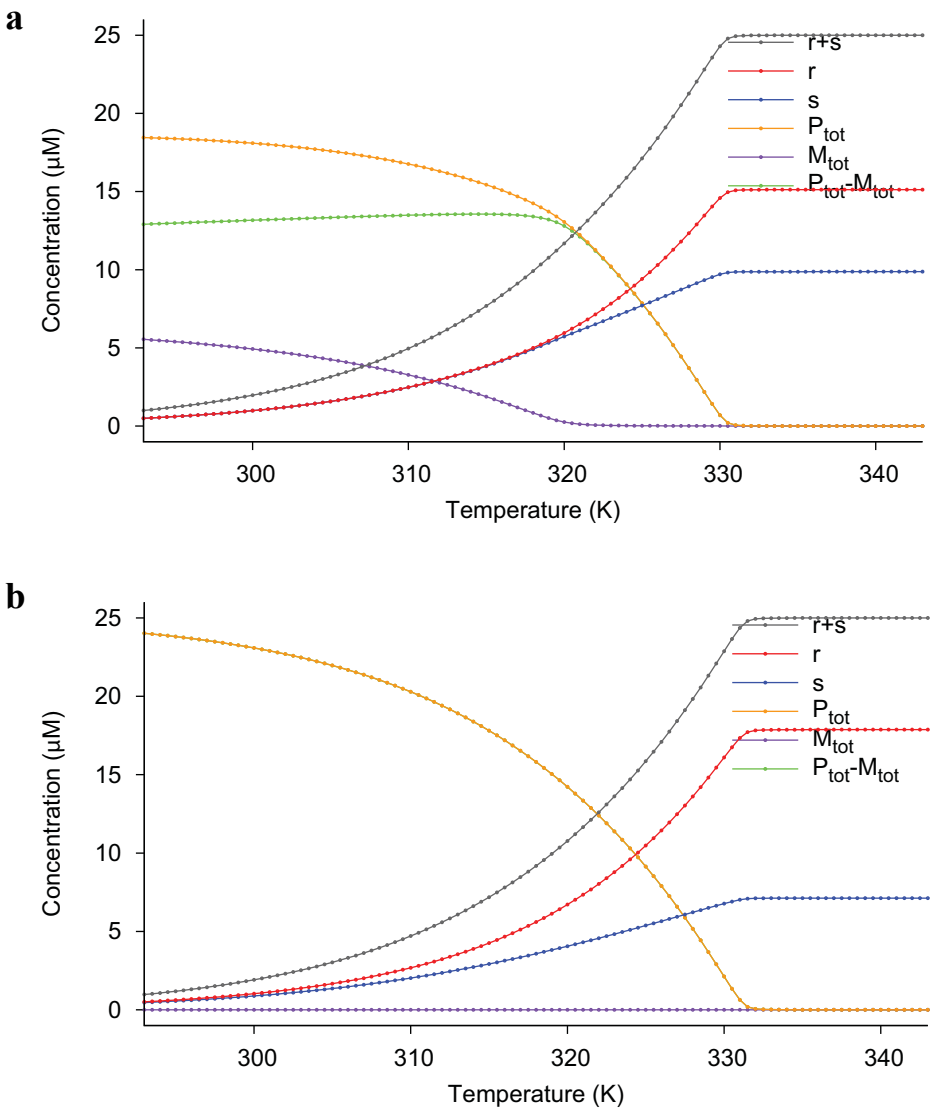

Supplementary Figure S3| Speciation plots of majority-rules melting curves (Fig 4d). The temperature-dependent monomer concentrations (r and s), concentration of BTA molecules belonging to *P*-type and *M*-type supramolecular polymers and their difference (P_{tot}-M_{tot}) for a total concentration of 2.5×10^{-5} M and two different values of the enantiomeric excess (*ee*), i.e., (**a**) *ee*=0.21 and (**b**) *ee*=0.43.

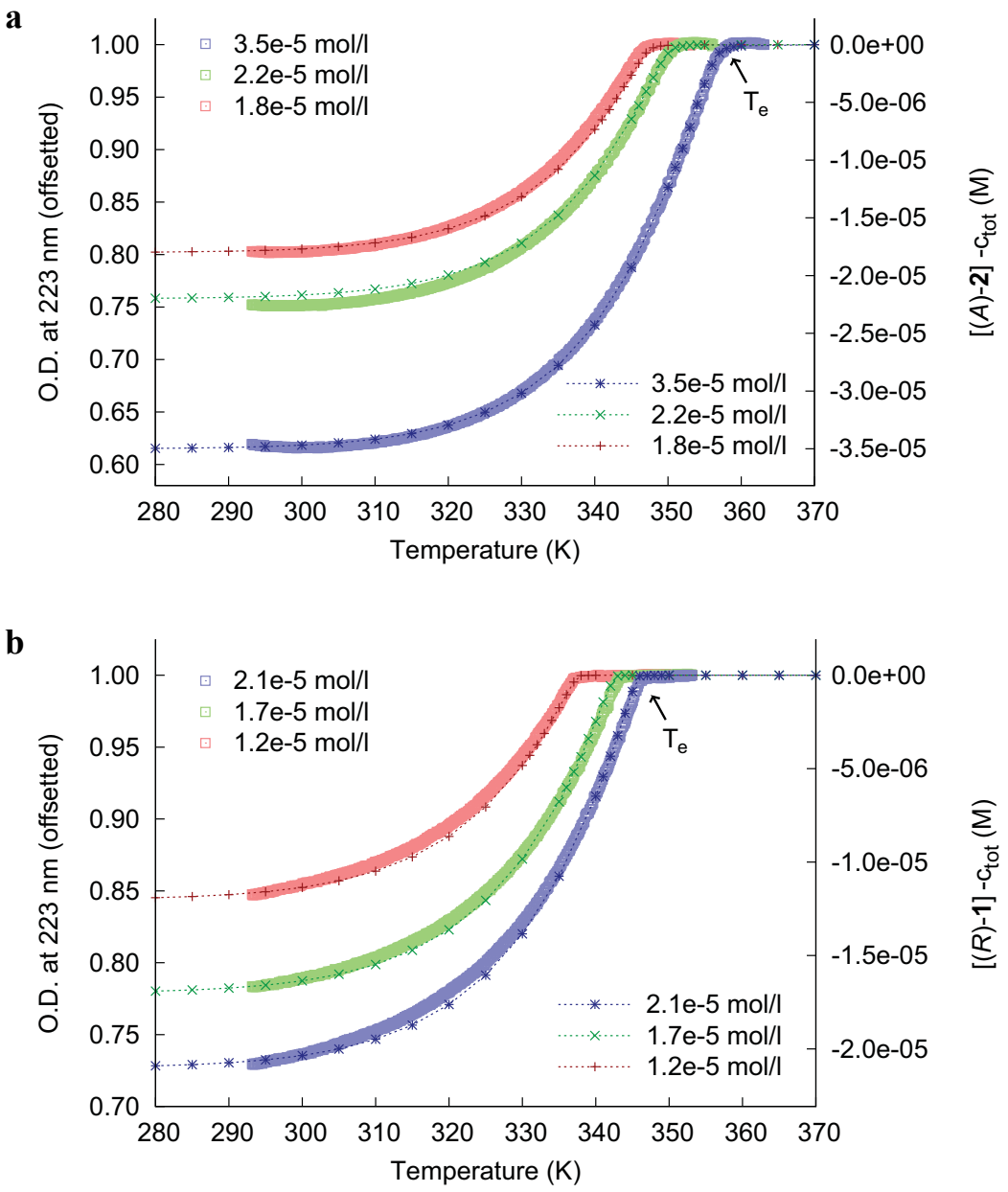

Supplementary Figure S4| Fit of experimental melting curves for (*R*)-1 and (*A*)-2 in heptane. Comparison of the experimentally determined optical density at 223 nm (light colored squares) as a function of temperature[27] to the total concentration of BTA molecules present in all oligomers and polymers with length two or higher simulated using the SSA (small symbols connected by broken lines) for (**a**) the soldiers (*A*)-**2** and (**b**) the sergeants (*R*)-**1**. The elongation temperature, T_e, is defined as the critical temperature separating the nucleation and elongation regime. The experimental curves are displayed using an offset for clarity.

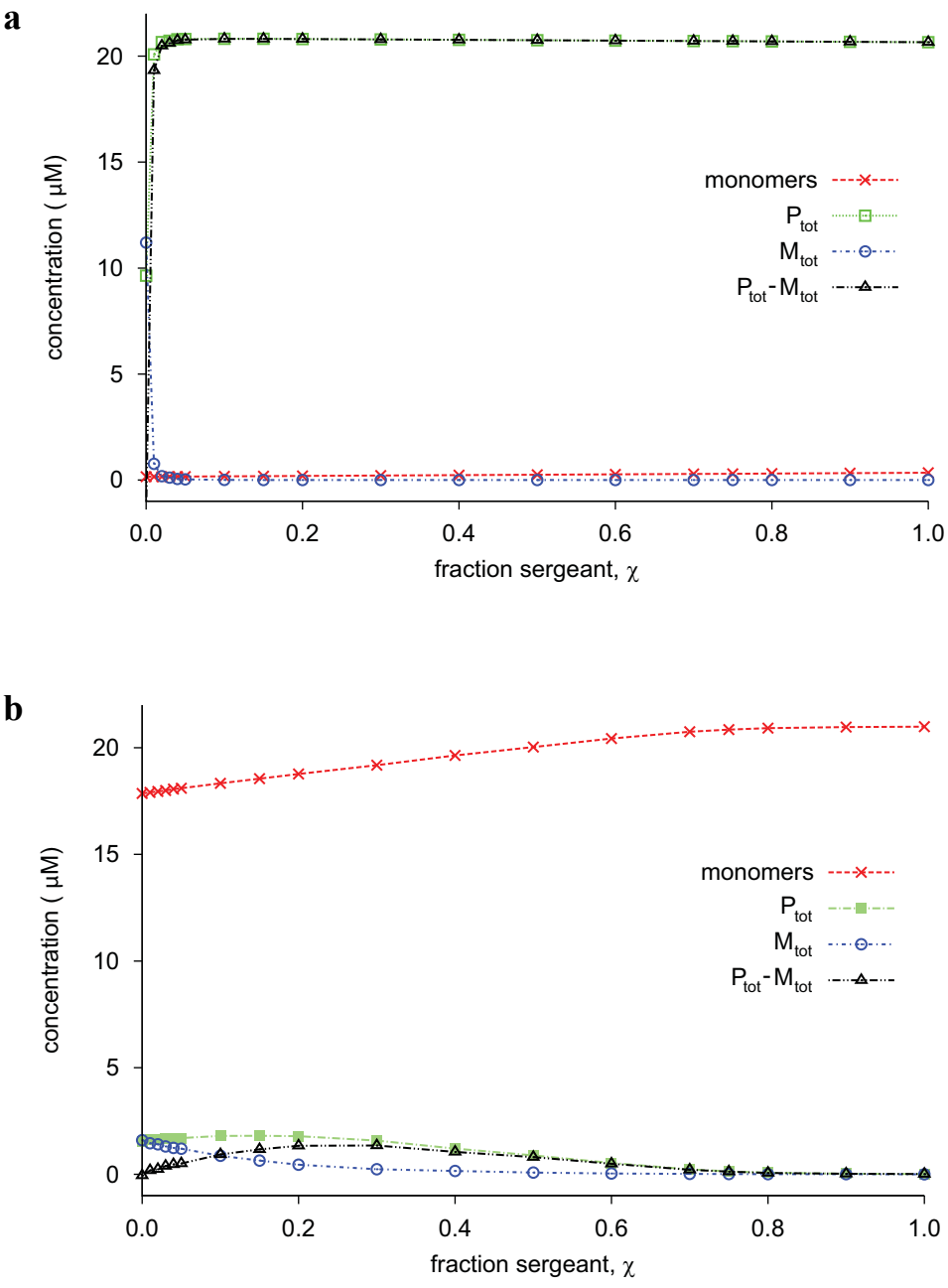

Supplementary Figure S5| Speciation plots for sergeants-and-soldiers. Total monomer concentration, concentration of BTA molecules belonging to *P* and *M*-type supramolecular polymers and their difference (P_{tot}-M_{tot}) as a function of the mole fraction sergeant (χ) for a total concentration of 2.1×10^{-5} M at two different temperatures, i.e., (**a**) T = 293 K and (**b**) T = 347 K.

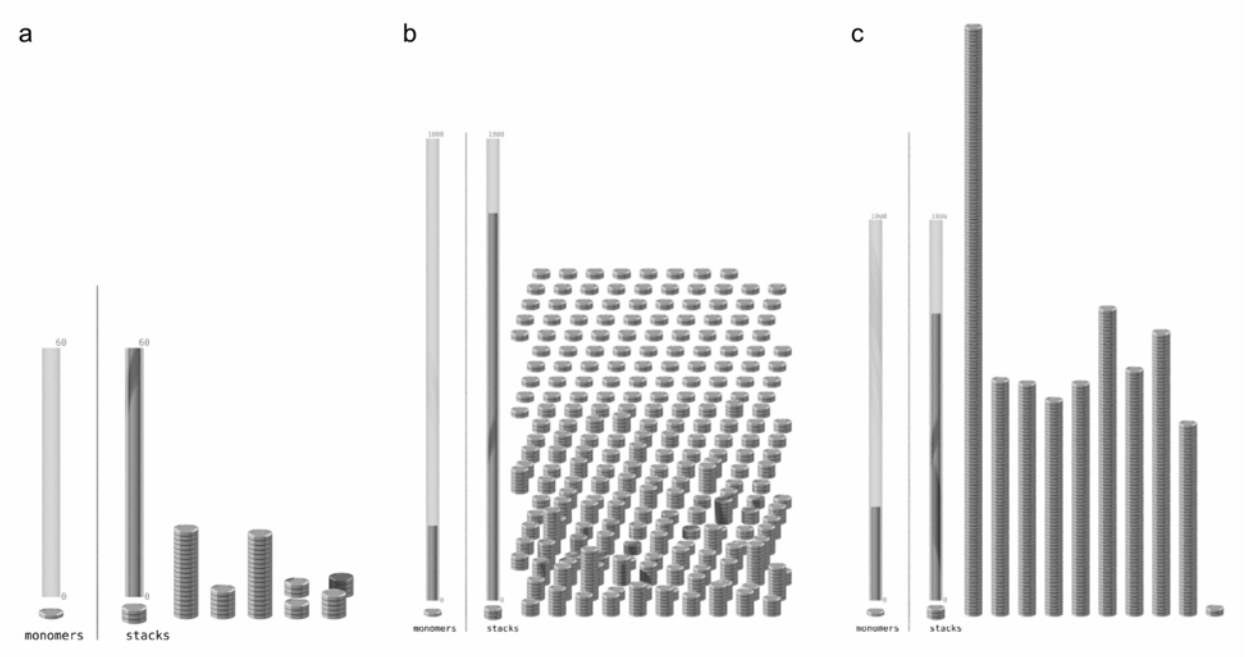

Supplementary Figure S6: Snapshots of three movies demonstrating the simulation approach and the difference between isodesmic and cooperative supramolecular polymerization. In the movies all supramolecular polymers are visualized individually. Next to these polymers a bar shows the total amount of molecules in supramolecular polymers. The monomers are not all shown individually, but the amount of monomers present is indicated by the bar at the left hand side of the movie. (**a**) Movie 1: Simulation of an isodesmic supramolecular polymerization of only 60 molecules, at dimensionless concentration Kc_{tot}=100, showing each reaction individually. (**b**) Movie 2: Simulation of an isodesmic supramolecular polymerization of 1000 molecules at concentration Kc_{tot}=4. (**c**) Movie 3: Simulation of a nucleation-elongation supramolecular polymerization, with nucleus size 2 and nucleation factor $\sigma=2\times10^{-5}$, of 1000 molecules at concentration Kc_{tot}=4. The latter two movies clearly show the difference between an isodesmic supramolecular polymerization, where many short aggregates are formed, and a cooperative supramolecular polymerization, where fewer but longer supramolecular polymers are formed.

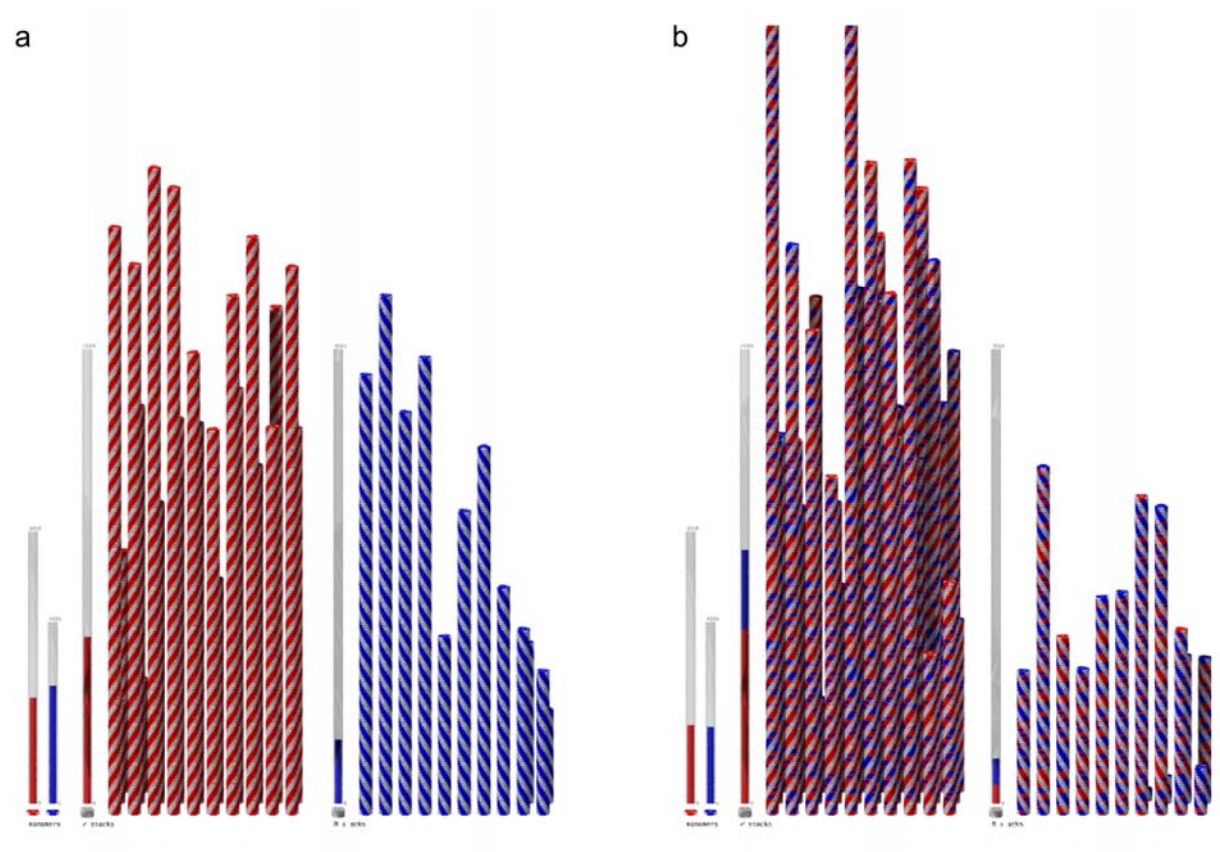

Supplementary Figure S7: Snapshots of two movies demonstrating the majority-rules effect. Whereas the first three movies contained only one monomer type forming a single type of supramolecular polymer, here supramolecular copolymerizations are considered where mixtures of two monomer types can form supramolecular polymers of two types of helicity (*P* and *M*-type). In the movies all supramolecular polymers are again visualized individually, also showing their helicity and *M*-type at the right hand side and *P*-type in the middle, whereas the amount of monomers of both types is shown using two bars at the left hand side. Both simulations contain 10,000 molecules, i.e. 6000 (*R*)-**1** molecules (red) that prefer the *P*-type helicity and 4000 (*S*)-**1** molecules (blue) that prefer *M*-type helicity, at a concentration of 2×10^{-5} mol/l and a temperature of 313 K and use the same thermodynamic parameters (as derived from fitting to the melting curves of BTA in MCH), except for the mismatch penalty. (**a**) Movie 4: With a high mismatch penalty (i.e., -30 kJ/mol) narcissistic[15] self-sorting of the two chiral components in stacks of opposite helicity takes place. (**b**) Movie 5: With a smaller mismatch penalty of -2.1 kJ/mol (as used in the article) social[15] self-sorting occurs and the majority-rules effect is clearly visible. Note that the conditions of this latter movie thus exactly correspond to those for speciation plot of Figure 4c of the article.

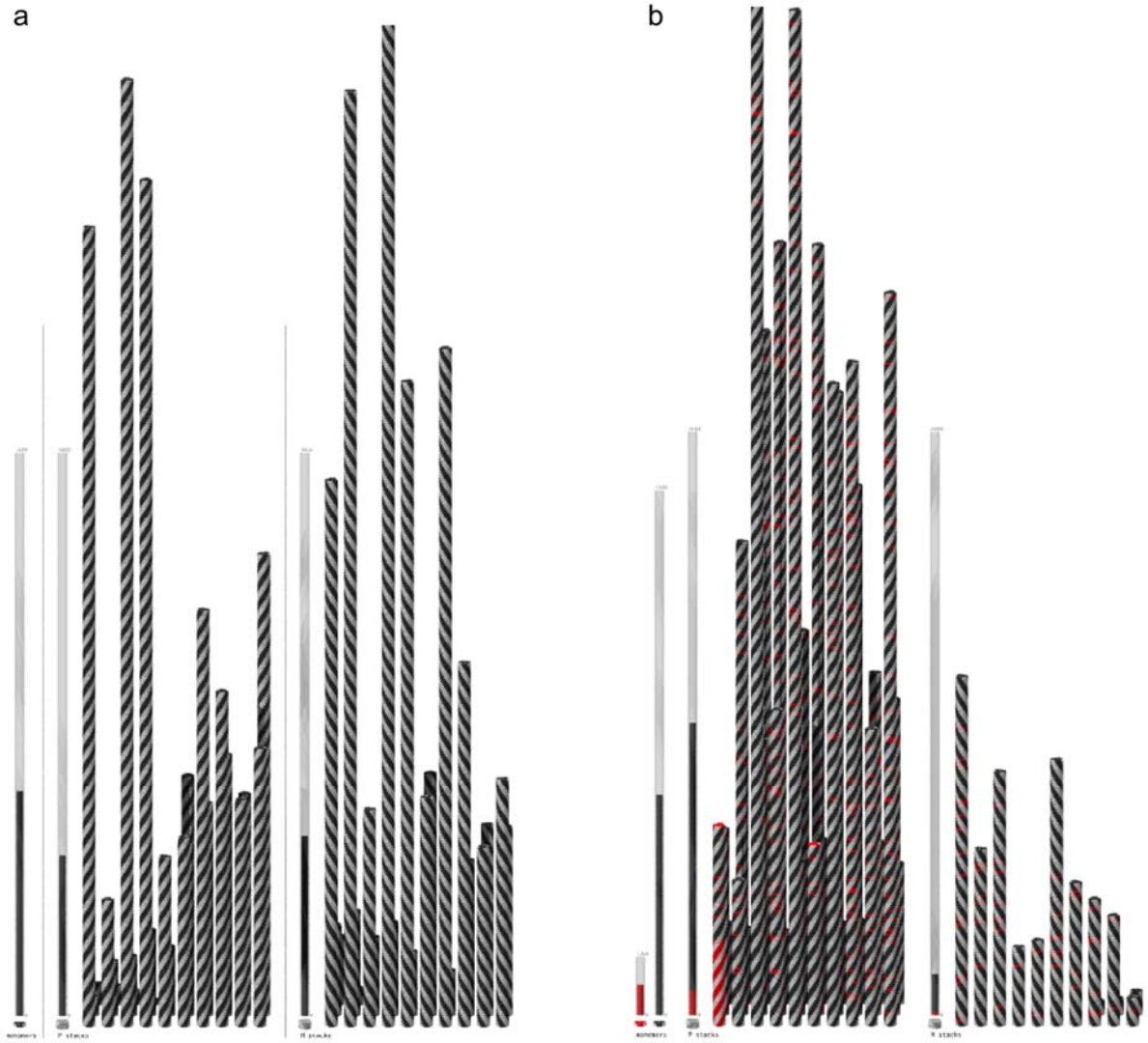

Supplementary Figure S8: Snapshots of two movies demonstrating the sergeants-and-soldiers effect. (**a**) Movie 6: 9000 achiral monomers ((*A*)-**2**, black) form supramolecular polymers of both *P* and *M*-type helicity in equal amounts. (**b**) Movie 7: With the addition of 10 percent sergeant ((*R*)-**1**, red) almost exclusively *P*-type supramolecular polymers are formed, clearly illustrating the sergeants-and-soldiers effect. Thermodynamic parameters for both movies are as derived from the melting curves of the BTA's in heptane and both simulations are performed at a concentration of 2.1×10-5 mol/l and a temperature of 337 K. Note that the conditions of these two movies thus exactly correspond to those for Figure 6c in the article.

Supplementary Methods

Parameter estimation from experimental melting curves

The values for the entropy change (ΔS^0 , $\Delta S^{0,A}$), enthalpy change (ΔH^0_{ELO} , $\Delta H^{0,A}_{ELO}$) and nucleation penalty (ΔH^0_{NP} , $\Delta H^{0,A}_{NP}$) as used in the cooperative supramolecular copolymerization models were obtained by fitting to the melting curves of the single-component systems. These melting curves where either obtained by temperature dependent circular dichroism (CD) or temperature dependent UV-vis spectroscopy. The entropy (ΔS^0 , $\Delta S^{0,A}$) and enthalpy (ΔH^0_{ELO} , $\Delta H^{0,A}_{ELO}$) changes were obtained by using a Van 't Hoff plot, where, for a number of melting curves at different concentrations, the natural logarithm of the concentration is plotted versus the reciprocal elongation temperature. From such a plot the enthalpy and entropy changes can then be obtained from the slope and the crossing with the x-axis, respectively, as for instance illustrated in Smulders et al[27] for the sergeants-and-soldiers system considered here. The nucleation penalty was then tuned to match the shape of the melting curve around the elongation temperature.

Majority-rules In the case of the majority-rules principle, experimentally determined CD intensity at 223 nm of solutions of (*R*)-**1** as a function of temperature for three different concentrations in methylcyclohexane (MCH) was used from Smulders et al.[28] The CD intensity at this wavelength is assumed to be a characteristic measure for the difference in material in *P* and *M*-type aggregates. Supplementary Figure S1 (left y-axis) depicts the experimental data. Supplementary Figure S1 (right y-axis) also displays the difference in material in *P* and *M*-type aggregates as a function of temperature as determined by the mass-balance model using a nucleus size of two, entropy increment $\Delta S^0 = -0.128$ kJ/mol/K, enthalpy increment $\Delta H^0_{ELO} = -72$ kJ/mol and nucleation penalty $\Delta H^0_{NP} = -30$ kJ/mol for the chiral (*R*)-**1** in MCH. As can be observed from Supplementary Figure S1, the mass-balance model describes the cooperative supramolecular polymerization of (*R*)-**1** in dilute solutions very well at all

concentrations considered using only three thermodynamic parameters (i.e., $\Delta H^0_{\mathrm{ELO}}$, ΔS^0, and ΔH^0_{NP}).

Sergeants-and-soldiers Because supramolecular polymerization of achiral (*A*)-**2** results in equal amounts of *P* and *M*-type supramolecular polymers, the temperature dependent aggregation cannot be probed by CD spectroscopy. Therefore, thermodynamic parameters were determined from UV-vis absorption data both for the achiral (soldier) as well as the chiral (sergeant) BTA's. Supplementary Figure S4 (left y-axis) depicts the experimentally determined change in the UV-vis absorption at 223 nm of solutions of pure (*A*)-**2** and pure (*R*)-**1** as a function of temperature for three different concentrations in heptane. We have previously shown that changes in the UV-vis absorption at this wavelength is a characteristic measure for the fraction of aggregation of monomeric (*A*)-**2** and (*R*)-**1** into hydrogen-bonded supramolecular polymers.[27] Supplementary Figure S4 (right y-axis) also displays the total concentration BTA molecules in all oligomers and polymers with length two or higher as a function of temperature determined by our SSA using a nucleus size of two, entropy increment $\Delta S^0 = -0.1015$ kJ/mol/K, enthalpy increment $\Delta H^0_{\mathrm{ELO}} = -66$ kJ/mol and nucleation penalty $\Delta H^0_{\mathrm{NP}} = -35$ kJ/mol for the chiral (*R*)-**1** and entropy increment $\Delta S^{0,\mathrm{A}} = -0.1255$ kJ/mol/K, enthalpy increment $\Delta H^{0,\mathrm{A}}_{\mathrm{ELO}} = -75$ kJ/mol and nucleation penalty $\Delta H^{0,\mathrm{A}}_{\mathrm{NP}} = -27$ kJ/mol for the achiral (*A*)-**2**. As can be observed from Supplementary Figure S4, our SSA describes the cooperative supramolecular polymerization of (*R*)-**1** and (*A*)-**2** in dilute solutions very well at all concentrations considered using only three thermodynamic parameters (i.e., $\Delta H^0_{\mathrm{ELO}}$, ΔS^0, and ΔH^0_{NP}) for each monomer type. An important difference in the supramolecular polymerization of (*R*)-**1** and (*A*)-**2** is the higher elongation temperature (T_{e}) of the latter reflecting the higher thermal stability of supramolecular polymers consisting of achiral (*A*)-**2**. Presumably, the lower thermal stability of supramolecular polymers consisting of (*R*)-**1** is a result of increased steric interactions due to the bulkier chiral side chains.